physica status solidi b
www.pss-b.com
basic solid state physics

A moving screw dislocation interacting with an imperfect piezoelectric bimaterial interface

X. Wang and **E. Pan**

University of Akron, Akron, OH 44039, USA

Received 30 November 2006, revised 9 January 2007, accepted 1 February 2007
Published online 7 March 2007

PACS 46.25.Hf, 61.72.Lk, 68.35.Ct, 77.65.Ly

Closed-form solutions in terms of exponential integrals are derived for a constantly moving screw dislocation in a piezoelectric bimaterial with an imperfect interface. The imperfect interface discussed here is mechanically compliant and dielectrically weakly (or highly) conducting. The electroelastic fields due to the moving dislocation, such as stresses, strains, electric displacements and electric fields, are obtained for this bimaterial. The solutions derived here are valid when the moving velocity of the screw dislocation is below the Bleustein–Gulyaev wave speeds of the two piezoelectric half-planes. This restriction is different from that in a perfectly bonded bimaterial where the moving velocity of the screw dislocation is below the piezoelectrically stiffened bulk shear wave speeds of the two piezoelectric half-planes. Numerical results are also presented to demonstrate the influence of the interface imperfection and the velocity of the moving dislocation on the electroelastic fields in the piezoelectric bimaterial.

phys. stat. sol. (b) **244**, No. 6, 1940–1956 (2007) / **DOI** 10.1002/pssb.200642586

WILEY-VCH

physica status solidi b

phys. stat. sol. (b) **244**, No. 6, 1940–1956 (2007) / **DOI** 10.1002/pssb.200642586

A moving screw dislocation interacting with an imperfect piezoelectric bimaterial interface

X. Wang and **E. Pan***

University of Akron, Akron, OH 44039, USA

Received 30 November 2006, revised 9 January 2007, accepted 1 February 2007
Published online 7 March 2007

PACS 46.25.Hf, 61.72.Lk, 68.35.Ct, 77.65.Ly

Closed-form solutions in terms of exponential integrals are derived for a constantly moving screw dislocation in a piezoelectric bimaterial with an imperfect interface. The imperfect interface discussed here is mechanically compliant and dielectrically weakly (or highly) conducting. The electroelastic fields due to the moving dislocation, such as stresses, strains, electric displacements and electric fields, are obtained for this bimaterial. The solutions derived here are valid when the moving velocity of the screw dislocation is below the Bleustein–Gulyaev wave speeds of the two piezoelectric half-planes. This restriction is different from that in a perfectly bonded bimaterial where the moving velocity of the screw dislocation is below the piezoelectrically stiffened bulk shear wave speeds of the two piezoelectric half-planes. Numerical results are also presented to demonstrate the influence of the interface imperfection and the velocity of the moving dislocation on the electroelastic fields in the piezoelectric bimaterial.

1 Introduction

Study of moving dislocations is important in material sciences and other areas. For instance, a moving dislocation induced stress can result in the local rearrangement of solute atoms [1]. Its density and velocity are closely related to the plastic deformation of the crystal [2]. A moving dislocation in the defect structure can also introduce dislocation multiplication behind it [3], and its velocity in a crystal can be changed due to the lattice periodicity [4]. Recently moving dislocation problems in piezoelectric solids have attracted much attention. Wang and Zhong [5] derived explicit expressions of electroelastic fields induced by a moving screw dislocation in a transversely isotropic piezoelectric material. Wu et al. [6] addressed the problem of a moving screw dislocation in a piezoelectric bimaterial. Some errors in the paper of Wu et al. [6] were found and corrected by Liu and Fang [7]. The steady-state version of the Stroh formalism for piezoelectricity was employed by Soh et al. [8] to derive closed-form solutions for a moving dislocation in an anisotropic piezoelectric solid. Making use of the full dynamic equations of piezoelectromagnetism, Yang [9] analyzed a moving screw dislocation in polarized ceramics.

When analyzing a moving dislocation in a piezoelectric bimaterial, it is assumed that the bimaterial interface is perfect, i.e., tractions, displacements, electric potential and normal electric displacement are all continuous across the interface (see [6, 7] for more details). The assumption of a perfect interface may be inadequate to account for the damage occurring on the interface (see, e.g., [10, 11]). Recently Wang and Sudak [12] discussed a static screw dislocation interacting with an imperfect interface in a piezoelectric bimaterial. Two types of imperfect interface were considered: (1) mechanically compliant and dielectrically weakly conducting interface; and (2) mechanically compliant and dielectrically highly conducting

* Corresponding author: e-mail: pan2@uakron.edu, Phone: 330-972-6739, Fax: 330-972-6020

interface. For a mechanically compliant interface, tractions are continuous but elastic displacements are discontinuous across the imperfect interface; jumps in the displacement components are further assumed to be proportional, in terms of the 'spring-type' interface parameters, to their respective interface traction components. For a dielectrically weakly conducting interface, the normal electric displacement is continuous but the electric potential is discontinuous across the interface; jump in the electric potential is proportional to the normal electric displacement. For a dielectrically highly conducting interface, the electric potential is continuous across the interface whereas the normal electric displacement experiences a discontinuity across the interface, which is proportional to the differential expression of the electric potential. It is found in [12] that two parameters are needed to describe the interface "rigidity". Fan et al. [13] found that certain waves exist, which propagate near an imperfectly bonded interface between two half-spaces of different piezoelectric ceramics.

The aim of this research is to find the electroelastic field due to a moving screw dislocation in a piezoelectric bimaterial with an imperfect interface. As in the static case [12], two kinds of imperfect interfaces are considered: (1) mechanically compliant and dielectrically weakly conducting; and (2) mechanically compliant and dielectrically highly conducting. In Section 2 we present two versions of the complex variable formulations which are suitable for treating the two kinds of imperfect interfaces, respectively. The field potentials for these two imperfect interface cases are derived in Section 3. Numerical results are presented in Section 4. Conclusions are drawn in Section 5.

2 Basic formation

Shown in Fig. 1 are two dissimilar piezoelectric half-planes, which are bonded together at the interface $x_2 = 0$. Both the upper half plane, denoted by #1, and the lower half plane, denoted by #2, are transversely isotropic with the poling direction parallel to the x_3-axis. Consider a screw dislocation moving at a constant velocity V along the x_1'-axis within the upper half-plane (the x_1'-axis is parallel to the x_1-axis, and the distance between the two parallel axes is δ). The screw dislocation is assumed to be straight and infinitely long in the x_3-direction, experiencing a displacement jump b and an electric potential jump $\Delta\phi$ across the slip plane. Throughout this paper, the subscripts 1 and 2 to vectors or matrices and the superscripts (1) and (2) to the field components are used to identify the quantities in the upper and lower half-planes, respectively.

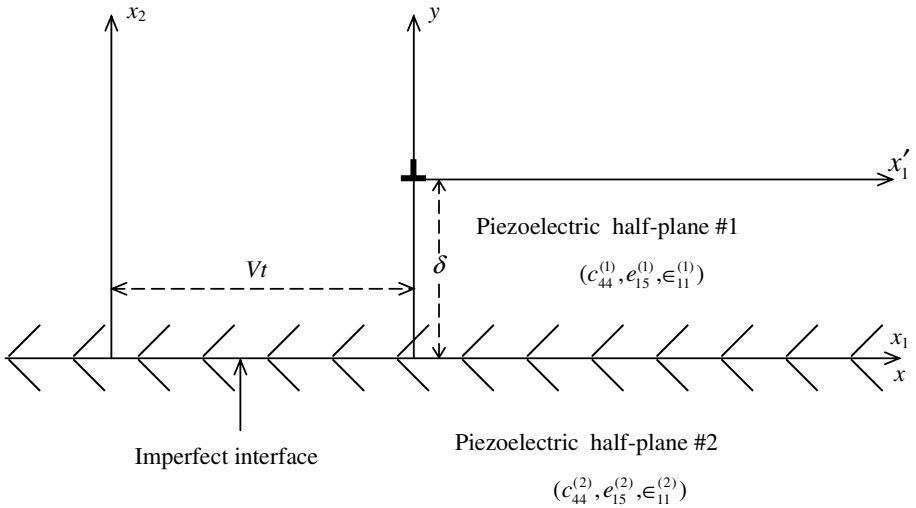

Fig. 1 A moving screw dislocation interacting with an imperfect interface in a piezoelectric bimaterial.

In the absence of body forces and electric charges, the governing equations are

$$\sigma_{31,1} + \sigma_{32,2} = \rho \frac{\partial^2 w}{\partial t^2}, \qquad D_{1,1} + D_{2,2} = 0, \tag{1}$$

where a comma followed by 1 (or 2) denotes partial derivatives with respect to x_1 (or x_2); σ_{31} and σ_{32} are the stress components; D_1 and D_2 are the electric displacements; ρ is the mass density; w is the out-of-plane displacement.

The linear, piezoelectric constitutive equations for a transversely isotropic piezoelectric material poled along the x_3-axis are given by

$$\begin{bmatrix} \sigma_{32} \\ D_2 \end{bmatrix} = \begin{bmatrix} c_{44} & -e_{15} \\ e_{15} & \varepsilon_{11} \end{bmatrix} \begin{bmatrix} w_{,2} \\ E_2 \end{bmatrix}, \tag{2a}$$

$$\begin{bmatrix} \sigma_{31} \\ D_1 \end{bmatrix} = \begin{bmatrix} c_{44} & -e_{15} \\ e_{15} & \varepsilon_{11} \end{bmatrix} \begin{bmatrix} w_{,1} \\ E_1 \end{bmatrix}, \tag{2b}$$

where E_1 and E_2 are the electric fields; c_{44}, e_{15} and ε_{11} are, respectively, the elastic modulus, piezoelectric constant and dielectric permittivity. The electric fields E_1 and E_2 can be obtained from the electric potential ϕ as follows

$$E_1 = -\phi_{,1}, \qquad E_2 = -\phi_{,2}. \tag{3}$$

The boundary conditions on a compliant and weakly conducting interface are given by

$$\begin{aligned} &\sigma_{32}^{(1)} = \sigma_{32}^{(2)}, \qquad D_2^{(1)} = D_2^{(2)}, \\ &w^{(1)} - w^{(2)} = \alpha \sigma_{32}^{(2)}, \qquad \phi^{(1)} - \phi^{(2)} = -\beta D_2^{(2)}, \end{aligned} \qquad x_2 = 0 \tag{4}$$

where the two interface parameters α and β are nonnegative constants. The special case $\alpha = \beta = 0$ corresponds to a perfect interface, whereas $\alpha, \beta \to \infty$ describes a completely debonded and charge-free (insulating) interface.

The boundary conditions on a compliant and highly conducting interface are given by

$$\begin{aligned} &\sigma_{32}^{(1)} = \sigma_{32}^{(2)}, \qquad E_1^{(1)} = E_1^{(2)}, \\ &w^{(1)} - w^{(2)} = \chi \sigma_{32}^{(2)}, \qquad D_2^{(1)} - D_2^{(2)} = \gamma \frac{\partial^2 \phi^{(2)}}{\partial x_1^2}, \end{aligned} \qquad x_2 = 0, \tag{5}$$

where the two interface parameters χ and γ are nonnegative constants. The special case $\chi = \gamma = 0$ corresponds to a perfect interface, whereas $\chi, \gamma \to \infty$ describes a completely debonded and equipotential interface.

To facilitate the analysis of the problem, we choose a new coordinate system (x, y, x_3) which moves at the same velocity V as the screw dislocation The moving and fixed coordinate systems coincide at time $t = 0$. We make the following Galilean transformation between the fixed (x_1, x_2, x_3) and moving (x, y, x_3) coordinate systems

$$x = x_1 - Vt, \qquad y = x_2, \qquad x_3 = x_3, \tag{6}$$

In the moving coordinate system, the dislocation is located at $x = 0,\ y = \delta$. All of the field components are not explicitly dependent on the time t in the moving coordinate system. In addition we define the parameter η as

$$\eta = \sqrt{1 - V^2/s^2}, \tag{7}$$

where $s = \sqrt{\tilde{c}_{44}/\rho}$ is the speed of the piezoelectrically stiffened bulk shear wave with $\tilde{c}_{44} = c_{44} + e_{15}^2/\varepsilon_{11}$ being the piezoelectrically stiffened elastic constant. In the following we will present two complex variable formulations [14, 15] which are suitable for treating the two kinds of imperfect interfaces, respectively.

2.1 Complex variable formulation for a compliant and weakly conducting interface

The displacement and electric potential can be expressed in terms of an analytic function vector $\boldsymbol{f}(z) = [f_1(z_1) \quad f_2(z)]^T$, $(z_1 = x + i\eta y,\ z = x + iy)$ as [5]

$$\boldsymbol{U} = \begin{bmatrix} w \\ \phi \end{bmatrix} = \boldsymbol{A}\,\mathrm{Im}\{\boldsymbol{f}(z)\}, \tag{8}$$

where $\boldsymbol{U}$ can be termed as the generalized displacement vector, and the 2×2 real matrix $\boldsymbol{A}$ is

$$\boldsymbol{A} = \begin{bmatrix} 1 & 0 \\ \dfrac{e_{15}}{\varepsilon_{11}} & 1 \end{bmatrix}. \tag{9}$$

The stresses and electric displacements can also be expressed in terms of $\boldsymbol{f}(z)$ as

$$\begin{bmatrix} \sigma_{32} \\ D_2 \end{bmatrix} = \mathrm{Re}\{\boldsymbol{B}\boldsymbol{f}'(z)\}, \qquad \begin{bmatrix} \sigma_{31} \\ D_1 \end{bmatrix} = \mathrm{Im}\{\boldsymbol{C}\boldsymbol{f}'(z)\}, \tag{10}$$

where the two 2×2 matrices $\boldsymbol{B}$ and $\boldsymbol{C}$ are

$$\boldsymbol{B} = \begin{bmatrix} \eta\tilde{c}_{44} & e_{15} \\ 0 & -\varepsilon_{11} \end{bmatrix}, \qquad \boldsymbol{C} = \begin{bmatrix} \tilde{c}_{44} & e_{15} \\ 0 & -\varepsilon_{11} \end{bmatrix}. \tag{11}$$

If we introduce a generalized stress function vector $\boldsymbol{\Phi}$ as [14, 15]

$$\begin{bmatrix} \sigma_{32} \\ D_2 \end{bmatrix} = \boldsymbol{\Phi}_{,x}, \qquad \begin{bmatrix} \sigma_{31} - \rho V^2 w_{,x} \\ D_1 \end{bmatrix} = -\boldsymbol{\Phi}_{,y}, \tag{12}$$

then $\boldsymbol{\Phi}$ can be expressed in terms of $\boldsymbol{f}(z)$ as

$$\boldsymbol{\Phi} = \mathrm{Re}\{\boldsymbol{B}\boldsymbol{f}(z)\}. \tag{13}$$

2.2 Complex variable formulation for a compliant and highly conducting interface

We first introduce a function φ which is related to the electric displacements through

$$D_2 = \varphi_{,x}, \qquad D_1 = -\varphi_{,y}. \tag{14}$$

The generalized displacement vector $\boldsymbol{U} = [w \quad \varphi]^T$ can then be expressed in terms of an analytic function vector $\boldsymbol{f}(z) = [f_1(z_1) \quad f_2(z)]^T$ as [16]

$$\boldsymbol{U} = \begin{bmatrix} w \\ \varphi \end{bmatrix} = \boldsymbol{A}\,\mathrm{Im}\{\boldsymbol{f}(z)\}, \tag{15}$$

where the 2×2 real matrix $\boldsymbol{A}$ is an identity matrix,

$$\boldsymbol{A}=\begin{bmatrix}1 & 0\\ 0 & 1\end{bmatrix}. \tag{16}$$

The stresses and electric fields can also be expressed in terms of $\boldsymbol{f}(z)$ as

$$\begin{bmatrix}\sigma_{32}\\ -E_1\end{bmatrix}=\mathrm{Re}\{\boldsymbol{B}\boldsymbol{f}'(z)\},\qquad \begin{bmatrix}\sigma_{31}\\ E_2\end{bmatrix}=\mathrm{Im}\{\boldsymbol{C}\boldsymbol{f}'(z)\}, \tag{17}$$

where the two 2×2 matrices $\boldsymbol{B}$ and $\boldsymbol{C}$ are

$$\boldsymbol{B}=\begin{bmatrix}\eta\tilde{c}_{44} & i\dfrac{e_{15}}{\varepsilon_{11}}\\ -i\dfrac{e_{15}}{\varepsilon_{11}} & \dfrac{1}{\varepsilon_{11}}\end{bmatrix},\qquad \boldsymbol{C}=\begin{bmatrix}\tilde{c}_{44} & i\dfrac{e_{15}}{\varepsilon_{11}}\\ -i\eta\dfrac{e_{15}}{\varepsilon_{11}} & \dfrac{1}{\varepsilon_{11}}\end{bmatrix}. \tag{18}$$

Next if we introduce a generalized stress function vector $\boldsymbol{\Phi}$ as

$$\begin{bmatrix}\sigma_{32}\\ -E_1\end{bmatrix}=\boldsymbol{\Phi}_{,x},\qquad \begin{bmatrix}\sigma_{31}-\rho V^2 w_{,x}\\ E_2\end{bmatrix}=-\boldsymbol{\Phi}_{,y}, \tag{19}$$

then $\boldsymbol{\Phi}$ can be expressed in terms of $\boldsymbol{f}(z)$ as

$$\boldsymbol{\Phi}=\mathrm{Re}\{\boldsymbol{B}\boldsymbol{f}(z)\}. \tag{20}$$

Apparently the second component of $\boldsymbol{\Phi}$ is in fact the electric potential ϕ.

It is observed from Eqs. (8), (13), (15) and (20) that the generalized displacement and stress function vectors can be expressed in the same way in terms of $\boldsymbol{f}(z)$, $\boldsymbol{A}$ and $\boldsymbol{B}$ for the two kinds of imperfect interfaces. It has been verified [12] that the boundary conditions Eq. (4) for a compliant and weakly conducting interface and Eq. (5) for a compliant and highly conducting interface can both be commonly written in terms of the generalized displacement and stress function vectors $\boldsymbol{U}$ and $\boldsymbol{\Phi}$ as follows

$$\boldsymbol{\Phi}_1=\boldsymbol{\Phi}_2,\qquad \boldsymbol{U}_1-\boldsymbol{U}_2=\boldsymbol{\Lambda}\frac{\partial\boldsymbol{\Phi}_2}{\partial x},\qquad y=0, \tag{21}$$

where $\boldsymbol{\Lambda}=\mathrm{diag}[\alpha,-\beta]$ for a compliant and weakly conducting interface, and $\boldsymbol{\Lambda}=\mathrm{diag}[\chi,\gamma]$ for a compliant and highly conducting interface. In the following derivations, we will replace the complex variables $z_1=x+i\eta y$ by the common complex variable $z=x+iy$ due to the fact that $z_1=z$ on the real axis ($y=0$) [17]. When the analysis is finished, the complex variable $z=x+iy$ for $f_1(z)$ shall be changed back to the corresponding complex variable z_1.

3 Field potentials

The boundary conditions on the imperfect interface can be expressed in terms of the two analytic function vectors $\boldsymbol{f}_1(z)$ and $\boldsymbol{f}_2(z)$ as

$$\begin{aligned}&\boldsymbol{B}_1\boldsymbol{f}_1^{+}(x)+\overline{\boldsymbol{B}}_1\overline{\boldsymbol{f}}_1^{-}(x)=\boldsymbol{B}_2\boldsymbol{f}_2^{-}(x)+\overline{\boldsymbol{B}}_2\overline{\boldsymbol{f}}_2^{+}(x),\\ &\boldsymbol{A}_1\boldsymbol{f}_1^{+}(x)-\boldsymbol{A}_1\overline{\boldsymbol{f}}_1^{-}(x)-\boldsymbol{A}_2\boldsymbol{f}_2^{-}(x)+\boldsymbol{A}_2\overline{\boldsymbol{f}}_2^{+}(x)=i\boldsymbol{\Lambda}\left[\boldsymbol{B}_2\boldsymbol{f}_2'^{-}(x)+\overline{\boldsymbol{B}}_2\overline{\boldsymbol{f}}_2'^{+}(x)\right]\quad\text{on}\quad y=0.\end{aligned} \tag{22}$$

It follows from Eq. $(22)_1$ that

$$\begin{aligned} \boldsymbol{f}_1(z) &= \boldsymbol{B}_1^{-1}\overline{\boldsymbol{B}}_2\overline{\boldsymbol{f}}_2(z) + \boldsymbol{f}_0(z) - \boldsymbol{B}_1^{-1}\overline{\boldsymbol{B}}_1\overline{\boldsymbol{f}}_0(z)\,, \\ \overline{\boldsymbol{f}}_1(z) &= \overline{\boldsymbol{B}}_1^{-1}\boldsymbol{B}_2\boldsymbol{f}_2(z) - \overline{\boldsymbol{B}}_1^{-1}\boldsymbol{B}_1\boldsymbol{f}_0(z) + \overline{\boldsymbol{f}}_0(z)\,, \end{aligned} \tag{23}$$

where $\boldsymbol{f}_0(z)$ is the complex potential for a piezoelectric screw dislocation located at $x = 0$, $y = \delta$ in a homogeneous piezoelectric medium. The vector function $\boldsymbol{f}_0(z)$ can be easily determined by enforcing the following condition [8]

$$\oint_C \mathrm{d}\boldsymbol{U} = \hat{\boldsymbol{b}}\,, \qquad \oint_C \mathrm{d}\boldsymbol{\Phi} = \hat{\boldsymbol{f}}\,, \tag{24}$$

where C is any closed contour surrounding the dislocation core; $\hat{\boldsymbol{b}} = [b \quad \Delta\phi]^T$ and $\hat{\boldsymbol{f}} = 0$ for a compliant and weakly conducting interface; $\hat{\boldsymbol{b}} = [b \quad 0]^T$ and $\hat{\boldsymbol{f}} = [0 \quad \Delta\phi]^T$ for a compliant and highly conducting interface. When the interface is compliant and weakly conducting, $\boldsymbol{f}_0(z)$ is given by

$$\boldsymbol{f}_0(z) = \frac{1}{2\pi}\begin{bmatrix} b\ln(z - i\eta_1\delta) \\ \left(\Delta\phi - \dfrac{e_{15}^{(1)}}{\varepsilon_{11}^{(1)}}\, b\right)\ln(z - i\delta) \end{bmatrix}. \tag{25}$$

On the other hand, when the interface is compliant and highly conducting, $\boldsymbol{f}_0(z)$ is determined to be

$$\boldsymbol{f}_0(z) = \frac{1}{2\pi}\begin{bmatrix} b\ln(z - i\eta_1\delta) \\ i(e_{15}^{(1)}b - \varepsilon_{11}^{(1)}\,\Delta\phi)\ln(z - \mathrm{i}\delta) \end{bmatrix}. \tag{26}$$

Substituting the results of Eq. (23) into Eq. $(22)_2$, we can arrive at

$$\begin{aligned} &(\boldsymbol{A}_1\boldsymbol{B}_1^{-1} + \overline{\boldsymbol{A}}_2\overline{\boldsymbol{B}}_2^{-1})\,\overline{\boldsymbol{B}}_2\overline{\boldsymbol{f}}_2^{+}(x) - i\boldsymbol{\Lambda}\overline{\boldsymbol{B}}_2\overline{\boldsymbol{f}}_2'^{+}(x) - \boldsymbol{A}_1(\boldsymbol{I} + \boldsymbol{B}_1^{-1}\overline{\boldsymbol{B}}_1)\,\overline{\boldsymbol{f}}_0(x) \\ &= (\boldsymbol{A}_1\overline{\boldsymbol{B}}_1^{-1} + \boldsymbol{A}_2\boldsymbol{B}_2^{-1})\,\boldsymbol{B}_2\boldsymbol{f}_2^{-}(x) + i\boldsymbol{\Lambda}\boldsymbol{B}_2\boldsymbol{f}_2'^{-}(x) - \boldsymbol{A}_1(\boldsymbol{I} + \overline{\boldsymbol{B}}_1^{-1}\boldsymbol{B}_1)\,\boldsymbol{f}_0(x) \quad \text{on} \quad y = 0\,. \end{aligned} \tag{27}$$

It's apparent that the left-hand side of Eq. (27) is analytic in the upper half-plane, whilst the right-hand side of Eq. (27) is analytic in the lower half-plane. Consequently the continuity condition in Eq. (27) implies that the left- and right-hand sides of Eq. (27) are identically zero in the upper and lower half-planes, respectively. It then follows that

$$\boldsymbol{H}\boldsymbol{B}_2\boldsymbol{f}_2(z) + i\boldsymbol{\Lambda}\boldsymbol{B}_2\boldsymbol{f}_2'(z) = \boldsymbol{A}_1(\boldsymbol{I} + \overline{\boldsymbol{B}}_1^{-1}\boldsymbol{B}_1)\,\boldsymbol{f}_0(z)\,, \qquad y \le 0\,, \tag{28}$$

where $\boldsymbol{H} = \boldsymbol{A}_1\overline{\boldsymbol{B}}_1^{-1} + \boldsymbol{A}_2\boldsymbol{B}_2^{-1}$ is a 2×2 Hermitian matrix. The above equation is a set of coupled first-order differential equations for the analytic function vector $\boldsymbol{f}_2(z)$ defined in the lower half-plane which is free of singularity (the screw dislocation).

If the imperfect interface is compliant and weakly conducting, then it can be easily verified that

$$\boldsymbol{H} = \begin{bmatrix} H_{11} & H_{12} \\ H_{12} & -H_{22} \end{bmatrix}, \tag{29}$$

where the three real values H_{11}, H_{22}, H_{12} are explicitly given by

$$\begin{aligned} H_{11} &= \frac{1}{\eta^{(1)}\tilde{c}_{44}^{(1)}} + \frac{1}{\eta^{(2)}\tilde{c}_{44}^{(2)}}\,, \\ H_{22} &= \frac{c_{44}^{(1)} - (1-\eta^{(1)})\,\tilde{c}_{44}^{(1)}}{\eta^{(1)}\tilde{c}_{44}^{(1)}\varepsilon_{11}^{(1)}} + \frac{c_{44}^{(2)} - (1-\eta^{(2)})\,\tilde{c}_{44}^{(2)}}{\eta^{(2)}\tilde{c}_{44}^{(2)}\varepsilon_{11}^{(2)}}\,, \\ H_{12} &= \frac{e_{15}^{(1)}}{\eta^{(1)}\tilde{c}_{44}^{(1)}\varepsilon_{11}^{(1)}} + \frac{e_{15}^{(2)}}{\eta^{(2)}\tilde{c}_{44}^{(2)}\varepsilon_{11}^{(2)}}\,. \end{aligned} \tag{30}$$

On the other hand, if the imperfect interface is compliant and highly conducting, then it can also be verified that

$$\boldsymbol{H} = \begin{bmatrix} \tilde{H}_{11} & i\tilde{H}_{12} \\ -i\tilde{H}_{12} & \tilde{H}_{22} \end{bmatrix}, \tag{31}$$

where the three real values $\tilde{H}_{11}$, $\tilde{H}_{22}$, $\tilde{H}_{12}$ are explicitly given by

$$\begin{aligned} \tilde{H}_{11} &= \frac{1}{c_{44}^{(1)} - (1-\eta^{(1)})\,\tilde{c}_{44}^{(1)}} + \frac{1}{c_{44}^{(2)} - (1-\eta^{(2)})\,\tilde{c}_{44}^{(2)}}, \\ \tilde{H}_{22} &= \frac{\eta^{(1)}\tilde{c}_{44}^{(1)}\varepsilon_{11}^{(1)}}{c_{44}^{(1)} - (1-\eta^{(1)})\,\tilde{c}_{44}^{(1)}} + \frac{\eta^{(2)}\tilde{c}_{44}^{(2)}\varepsilon_{11}^{(2)}}{c_{44}^{(2)} - (1-\eta^{(2)})\,\tilde{c}_{44}^{(2)}}, \\ \tilde{H}_{12} &= \frac{e_{15}^{(1)}}{c_{44}^{(1)} - (1-\eta^{(1)})\,\tilde{c}_{44}^{(1)}} - \frac{e_{15}^{(2)}}{c_{44}^{(2)} - (1-\eta^{(2)})\,\tilde{c}_{44}^{(2)}}. \end{aligned} \tag{32}$$

Here we restrict our attention to the case in which the speed of the screw dislocation is lower than the Bleustein–Gulyaev wave speeds of the two half-planes, i.e., $V < \min\{c_{\mathrm{bg}}^{(1)}, c_{\mathrm{bg}}^{(2)}\}$ where $c_{\mathrm{bg}}^{(i)} = s^{(i)}\sqrt{1-(k_e^{(i)})^4}$ ($i = 1, 2$) are the Bleustein–Gulyaev wave speeds [18, 19] of the two half-planes with $k_e^{(i)} = \sqrt{((e_{15}^{(i)})^2/\tilde{c}_{44}^{(i)}\varepsilon_{11}^{(i)})}$ ($i = 1, 2$) being the electromechanical coupling factors. It can be easily verified that $H_{11} > 0$, $H_{22} > 0$ and $\tilde{H}_{11} > 0$, $\tilde{H}_{22} > 0$, $\tilde{H}_{11}\tilde{H}_{22} > \tilde{H}_{12}^2$ when $V < \min\left\{c_{\mathrm{bg}}^{(1)}, c_{\mathrm{bg}}^{(2)}\right\}$.

In order to solve Eq. (28), we consider the following eigenvalue problem

$$(\boldsymbol{H} - \lambda\boldsymbol{\Lambda})\,\boldsymbol{\xi} = 0. \tag{33}$$

Due to the fact that, when $V < \min\left\{c_{\mathrm{bg}}^{(1)}, c_{\mathrm{bg}}^{(2)}\right\}$, the structure of $\boldsymbol{H}$ is identical to their static counterpart [12], solutions to Eq. (33) can be obtained, by analogy, from the static solution in Wang and Sudak [12]. As summarized in [12], there exist two positive real eigenvalues or two complex conjugate eigenvalues with positive real parts if the interface is compliant and weakly conducting; there always exist two positive real eigenvalues if the interface is compliant and highly conducting. We denote the two eigenvalues of Eq. (33) as λ_1 and λ_2, with the corresponding eigenvectors as $\boldsymbol{\xi}_1$ and $\boldsymbol{\xi}_2$.

In order to decouple Eq. (28), we introduce the following transformation

$$\boldsymbol{B}_2\boldsymbol{f}_2(z) = [\boldsymbol{\xi}_1 \quad \boldsymbol{\xi}_2]\begin{bmatrix} h_1(z) \\ h_2(z) \end{bmatrix}, \tag{34}$$

where $h_1(z)$ and $h_2(z)$ are two new analytic functions.

In the following, we will use the decoupling method to solve the original partial differential equations for the two different kinds of imperfect interfaces.

3.1 Field potentials for a compliant and weakly conducting interface

In view of Eq. (34) and the orthogonal relations for the two eigenvectors [12], it is found that Eq. (28) can always be decoupled into the following two independent first-order differential equations for $h_1(z)$ and $h_2(z)$ no matter whether the two eigenvalues are real or complex conjugate

$$\begin{aligned} -i\lambda_1 h_1(z) + h_1'(z) &= -ik_{11}\ln(z - i\eta^{(1)}\delta) - ik_{12}\ln(z - i\delta), \\ -i\lambda_2 h_2(z) + h_2'(z) &= -ik_{21}\ln(z - i\eta^{(1)}\delta) - ik_{22}\ln(z - i\delta), \end{aligned} \tag{35}$$

where the four constants k_{11}, k_{12}, k_{21} and k_{22} are given by

$$\begin{aligned} k_{11} &= \frac{(\lambda_1\alpha - H_{11})\,[\varepsilon_{11}^{(1)}H_{12} + e_{15}^{(1)}(\lambda_1\alpha - H_{11})]\,b}{\pi\varepsilon_{11}^{(1)}[\alpha H_{12}^2 - \beta(\lambda_1\alpha - H_{11})^2]}, \qquad k_{12} = \frac{(\lambda_1\alpha - H_{11})^2\,(\varepsilon_{11}^{(1)}\,\Delta\phi - e_{15}^{(1)}b)}{\pi\varepsilon_{11}^{(1)}[\alpha H_{12}^2 - \beta(\lambda_1\alpha - H_{11})^2]}, \\ k_{21} &= \frac{H_{12}[\varepsilon_{11}^{(1)}H_{12} + e_{15}^{(1)}(\lambda_2\alpha - H_{11})]\,b}{\pi\varepsilon_{11}^{(1)}[\alpha H_{12}^2 - \beta(\lambda_2\alpha - H_{11})^2]}, \qquad k_{22} = \frac{H_{12}(\lambda_2\alpha - H_{11})\,(\varepsilon_{11}^{(1)}\,\Delta\phi - e_{15}^{(1)}b)}{\pi\varepsilon_{11}^{(1)}[\alpha H_{12}^2 - \beta(\lambda_2\alpha - H_{11})^2]}. \end{aligned} \tag{36}$$

In view of the fact that $\mathrm{Re}\,\{\lambda_i\} > 0$, $(i = 1, 2)$, the solutions of Eq. (35) can be expressed as

$$\begin{aligned} h_1'(z) &= ik_{11}\exp\left[i\lambda_1(z - i\eta^{(1)}\delta)\right]E_1\left[i\lambda_1(z - i\eta^{(1)}\delta)\right] + ik_{12}\exp\left[i\lambda_1(z - i\delta)\right]E_1\left[i\lambda_1(z - i\delta)\right], \\ h_2'(z) &= ik_{21}\exp\left[i\lambda_2(z - i\eta^{(1)}\delta)\right]E_1\left[i\lambda_2(z - i\eta^{(1)}\delta)\right] + ik_{22}\exp\left[i\lambda_2(z - i\delta)\right]E_1\left[i\lambda_2(z - i\delta)\right], \end{aligned} \tag{37}$$

where the exponential integral is defined by [20]

$$E_1(z) = \int_z^\infty \frac{e^{-t}}{t}\,\mathrm{d}t\,. \tag{38}$$

It should be stressed that if $\mathrm{Re}\,\{\lambda_i\} < 0$, the term $\exp(i\lambda_i z)$ is then an admissible homogeneous solution to Eq. (35). This will cause the non-uniqueness of the solution. We leave this rather complicated case for further discussion.

The original analytic function vectors $\boldsymbol{f}_1'(z)$ and $\boldsymbol{f}_2'(z)$ can be easily determined to be

$$\begin{aligned} \boldsymbol{f}_1'(z) = -i &\begin{bmatrix} \dfrac{\varepsilon_{11}^{(1)}H_{12} + e_{15}^{(1)}(\lambda_1\alpha - H_{11})}{\eta^{(1)}\tilde{c}_{44}^{(1)}\varepsilon_{11}^{(1)}(\lambda_1\alpha - H_{11})} & \dfrac{\varepsilon_{11}^{(1)}H_{12} + e_{15}^{(1)}(\lambda_2\alpha - H_{11})}{\eta^{(1)}\tilde{c}_{44}^{(1)}\varepsilon_{11}^{(1)}H_{12}} \\ -\dfrac{1}{\varepsilon_{11}^{(1)}} & \dfrac{H_{11} - \lambda_2\alpha}{\varepsilon_{11}^{(1)}H_{12}} \end{bmatrix} \\ &\times\begin{bmatrix} k_{11}\exp\left[-i\lambda_1(z + i\eta^{(1)}\delta)\right]E_1\left[-i\lambda_1(z + i\eta^{(1)}\delta)\right] + k_{12}\exp\left[-i\lambda_1(z + i\delta)\right]E_1\left[-i\lambda_1(z + i\delta)\right] \\ k_{21}\exp\left[-i\lambda_2(z + i\eta^{(1)}\delta)\right]E_1\left[-i\lambda_2(z + i\eta^{(1)}\delta)\right] + k_{22}\exp\left[-i\lambda_2(z + i\delta)\right]E_1\left[-i\lambda_2(z + i\delta)\right] \end{bmatrix} \\ &-\frac{1}{2\pi}\begin{bmatrix} \dfrac{b}{z + i\eta^{(1)}\delta} \\ \dfrac{\varepsilon_{11}^{(1)}\,\Delta\phi - e_{15}^{(1)}b}{\varepsilon_{11}^{(1)}(z + i\delta)} \end{bmatrix} + \frac{1}{2\pi}\begin{bmatrix} \dfrac{b}{z - i\eta^{(1)}\delta} \\ \dfrac{\varepsilon_{11}^{(1)}\,\Delta\phi - e_{15}^{(1)}b}{\varepsilon_{11}^{(1)}(z - i\delta)} \end{bmatrix}, \end{aligned} \tag{39}$$

$$\begin{aligned} \boldsymbol{f}_2'(z) = i &\begin{bmatrix} \dfrac{\varepsilon_{11}^{(2)}H_{12} + e_{15}^{(2)}(\lambda_1\alpha - H_{11})}{\eta^{(2)}\tilde{c}_{44}^{(2)}\varepsilon_{11}^{(2)}(\lambda_1\alpha - H_{11})} & \dfrac{\varepsilon_{11}^{(2)}H_{12} + e_{15}^{(2)}(\lambda_2\alpha - H_{11})}{\eta^{(2)}\tilde{c}_{44}^{(2)}\varepsilon_{11}^{(2)}H_{12}} \\ -\dfrac{1}{\in_{11}^{(2)}} & \dfrac{H_{11} - \lambda_2\alpha}{\varepsilon_{11}^{(2)}H_{12}} \end{bmatrix} \\ &\times\begin{bmatrix} k_{11}\exp\left[i\lambda_1(z - i\eta^{(1)}\delta)\right]E_1\left[i\lambda_1(z - i\eta^{(1)}\delta)\right] + k_{12}\exp\left[i\lambda_1(z - i\delta)\right]E_1\left[i\lambda_1(z - i\delta)\right] \\ k_{21}\exp\left[i\lambda_2(z - i\eta^{(1)}\delta)\right]E_1\left[i\lambda_2(z - i\eta^{(1)}\delta)\right] + k_{22}\exp\left[i\lambda_2(z - i\delta)\right]E_1\left[i\lambda_2(z - i\delta)\right] \end{bmatrix}. \end{aligned} \tag{40}$$

We remark that the above expressions of $\boldsymbol{f}_1'(z)$ and $\boldsymbol{f}_2'(z)$ are only valid along the real x-axis. However, it's not difficult to arrive at the full-field expressions of $\boldsymbol{f}_1'(z)$ and $\boldsymbol{f}_2'(z)$ which are listed in the appendix. We also point out that the last term in $\boldsymbol{f}_1'(z)$ is the singular part due to the screw dislocation

whilst the first two terms in $\boldsymbol{f}_1'(z)$ are the regular parts due to the existence of the compliant and weakly conducting interface. Once $\boldsymbol{f}_1'(z)$ and $\boldsymbol{f}_2'(z)$ are known, the stresses, strains, electric displacements and electric fields can be obtained easily. For example the traction and normal electric displacement along the compliant and weakly conducting interface are as follows

$$\sigma_{32} = \mathrm{Im}\left\{\begin{array}{l} \dfrac{H_{12}k_{11}}{H_{11}-\lambda_1\alpha}\exp\left[i\lambda_1(x-\mathrm{i}\eta^{(1)}\delta)\right]E_1\left[i\lambda_1(x-i\eta^{(1)}\delta)\right] \\ +\dfrac{H_{12}k_{12}}{H_{11}-\lambda_1\alpha}\exp\left[i\lambda_1(x-i\delta)\right]E_1\left[i\lambda_1(x-i\delta)\right] \\ -k_{21}\exp\left[i\lambda_2(x-i\eta^{(1)}\delta)\right]E_1\left[i\lambda_2(x-i\eta^{(1)}\delta)\right] \\ -k_{22}\exp\left[i\lambda_2(x-i\delta)\right]E_1\left[i\lambda_2(x-i\delta)\right] \end{array}\right\},$$

$$D_2 = \mathrm{Im}\left\{\begin{array}{l} -k_{11}\exp\left[i\lambda_1(x-i\eta^{(1)}\delta)\right]E_1\left[i\lambda_1(x-\mathrm{i}\eta^{(1)}\delta)\right] \\ -k_{12}\exp\left[i\lambda_1(x-i\delta)\right]E_1\left[i\lambda_1(x-i\delta)\right] \\ +\dfrac{(H_{11}-\lambda_2\alpha)k_{21}}{H_{12}}\exp\left[i\lambda_2(x-i\eta^{(1)}\delta)\right]E_1\left[i\lambda_2(x-i\eta^{(1)}\delta)\right] \\ +\dfrac{(H_{11}-\lambda_2\alpha)k_{22}}{H_{12}}\exp\left[i\lambda_2(x-i\delta)\right]E_1\left[i\lambda_2(x-i\delta)\right] \end{array}\right\}, \quad \text{on} \quad y=0. \tag{41}$$

3.2 Field potentials for a compliant and highly conducting interface

In view of Eq. (34) and the orthogonal relations for the two eigenvectors [12], Eq. (28) can be decoupled into the following two independent first-order differential equations for $h_1(z)$ and $h_2(z)$ as

$$\begin{aligned} -i\lambda_1 h_1(z) + h_1'(z) &= -it_{11}\ln(z-i\eta^{(1)}\delta) - it_{12}\ln(z-i\delta), \\ -i\lambda_2 h_2(z) + h_2'(z) &= -t_{21}\ln(z-i\eta^{(1)}\delta) - t_{22}\ln(z-i\delta), \end{aligned} \tag{42}$$

where the four real constants t_{11}, t_{12}, t_{21} and t_{22} are given by

$$\begin{aligned} t_{11} &= \frac{\eta^{(1)}\tilde{c}_{44}^{(1)}(\lambda_1\chi-\tilde{H}_{11})[\tilde{H}_{12}+e_{15}^{(1)}(\lambda_1\chi-\tilde{H}_{11})]b}{\pi[c_{44}^{(1)}-(1-\eta^{(1)})\tilde{c}_{44}^{(1)}][\chi\tilde{H}_{12}^2+\gamma(\lambda_1\chi-\tilde{H}_{11})^2]}, \\ t_{12} &= \frac{(\lambda_1\chi-\tilde{H}_{11})[e_{15}^{(1)}\tilde{H}_{12}+\eta^{(1)}\tilde{c}_{44}^{(1)}\varepsilon_{11}^{(1)}(\lambda_1\chi-\tilde{H}_{11})](\varepsilon_{11}^{(1)}\Delta\phi-e_{15}^{(1)}b)}{\pi\varepsilon_{11}^{(1)}[c_{44}^{(1)}-(1-\eta^{(1)})\tilde{c}_{44}^{(1)}][\chi\tilde{H}_{12}^2+\gamma(\lambda_1\chi-\tilde{H}_{11})^2]}, \\ t_{21} &= \frac{\eta^{(1)}\tilde{c}_{44}^{(1)}\tilde{H}_{12}[\tilde{H}_{12}+e_{15}^{(1)}(\lambda_2\chi-\tilde{H}_{11})]b}{\pi[c_{44}^{(1)}-(1-\eta^{(1)})\tilde{c}_{44}^{(1)}][\chi\tilde{H}_{12}^2+\gamma(\lambda_2\chi-\tilde{H}_{11})^2]}, \\ t_{22} &= \frac{\tilde{H}_{12}[e_{15}^{(1)}\tilde{H}_{12}+\eta^{(1)}\tilde{c}_{44}^{(1)}\varepsilon_{11}^{(1)}(\lambda_2\chi-\tilde{H}_{11})](\varepsilon_{11}^{(1)}\Delta\phi-e_{15}^{(1)}b)}{\pi\varepsilon_{11}^{(1)}[c_{44}^{(1)}-(1-\eta^{(1)})\tilde{c}_{44}^{(1)}][\chi\tilde{H}_{12}^2+\gamma(\lambda_2\chi-\tilde{H}_{11})^2]}, \end{aligned} \tag{43}$$

In view of the fact that $\lambda_i > 0$, $(i = 1, 2)$, the solutions of Eq. (42) can be given by

$$\begin{aligned} h_1'(z) &= it_{11}\exp\left[i\lambda_1(z-i\eta^{(1)}\delta)\right]E_1\left[i\lambda_1(z-i\eta^{(1)}\delta)\right] + it_{12}\exp\left[i\lambda_1(z-i\delta)\right]E_1\left[i\lambda_1(z-i\delta)\right], \\ h_2'(z) &= t_{21}\exp\left[i\lambda_2(z-i\eta^{(1)}\delta)\right]E_1\left[i\lambda_2(z-i\eta^{(1)}\delta)\right] + t_{22}\exp\left[i\lambda_2(z-i\delta)\right]E_1\left[i\lambda_2(z-i\delta)\right]. \end{aligned} \tag{44}$$

The original analytic function vectors $\boldsymbol{f}_1'(z)$ and $\boldsymbol{f}_2'(z)$ can then be easily determined to be

$$\boldsymbol{f}_1'(z)=\begin{bmatrix} \dfrac{\tilde{H}_{12}+e_{15}^{(1)}(\lambda_1\chi-\tilde{H}_{11})}{(\lambda_1\chi-\tilde{H}_{11})\left[c_{44}^{(1)}-(1-\eta^{(1)})\,\tilde{c}_{44}^{(1)}\right]} & -i\dfrac{\tilde{H}_{12}+e_{15}^{(1)}(\lambda_2\chi-\tilde{H}_{11})}{\tilde{H}_{12}\left[c_{44}^{(1)}-(1-\eta^{(1)})\,\tilde{c}_{44}^{(1)}\right]} \\ i\dfrac{e_{15}^{(1)}\tilde{H}_{12}+\eta^{(1)}\tilde{c}_{44}^{(1)}\varepsilon_{11}^{(1)}(\lambda_1\chi-\tilde{H}_{11})}{(\lambda_1\chi-\tilde{H}_{11})\left[c_{44}^{(1)}-(1-\eta^{(1)})\,\tilde{c}_{44}^{(1)}\right]} & \dfrac{e_{15}^{(1)}\tilde{H}_{12}+\eta^{(1)}\tilde{c}_{44}^{(1)}\varepsilon_{11}^{(1)}(\lambda_2\chi-\tilde{H}_{11})}{\tilde{H}_{12}\left[c_{44}^{(1)}-(1-\eta^{(1)})\,\tilde{c}_{44}^{(1)}\right]} \end{bmatrix}$$
$$\times\begin{bmatrix} -it_{11}\exp\left[-i\lambda_1(z+\mathrm{i}\eta^{(1)}\delta)\right]E_1\left[-i\lambda_1(z+i\eta^{(1)}\delta)\right]-it_{12}\exp\left[-i\lambda_1(z+i\delta)\right]E_1\left[-i\lambda_1(z+i\delta)\right] \\ t_{21}\exp\left[-i\lambda_2(z+\mathrm{i}\eta^{(1)}\delta)\right]E_1\left[-i\lambda_2(z+i\eta^{(1)}\delta)\right]+t_{22}\exp\left[-i\lambda_2(z+i\delta)\right]E_1\left[-i\lambda_2(z+i\delta)\right] \end{bmatrix}$$
$$-\frac{1}{2\pi}\begin{bmatrix} \dfrac{(1+\eta^{(1)})\,\tilde{c}_{44}^{(1)}-c_{44}^{(1)}}{c_{44}^{(1)}-(1-\eta^{(1)})\,\tilde{c}_{44}^{(1)}} & \dfrac{-2ie_{15}^{(1)}}{\varepsilon_{11}^{(1)}\left[c_{44}^{(1)}-(1-\eta^{(1)})\,\tilde{c}_{44}^{(1)}\right]} \\ \dfrac{2i\eta^{(1)}\tilde{c}_{44}^{(1)}e_{15}^{(1)}}{c_{44}^{(1)}-(1-\eta^{(1)})\,\tilde{c}_{44}^{(1)}} & \dfrac{(1+\eta^{(1)})\,\tilde{c}_{44}^{(1)}-c_{44}^{(1)}}{c_{44}^{(1)}-(1-\eta^{(1)})\,\tilde{c}_{44}^{(1)}} \end{bmatrix}\begin{bmatrix} \dfrac{b}{z+i\eta^{(1)}\delta} \\ \dfrac{i(\varepsilon_{11}^{(1)}\Delta\phi-e_{15}^{(1)}b)}{z+i\delta} \end{bmatrix}+\frac{1}{2\pi}\begin{bmatrix} \dfrac{b}{z-i\eta^{(1)}\delta} \\ \dfrac{i(e_{15}^{(1)}b-\varepsilon_{11}^{(1)}\Delta\phi)}{z-i\delta} \end{bmatrix}, \tag{45}$$

$$\boldsymbol{f}_2'(z)=\begin{bmatrix} \dfrac{\tilde{H}_{12}-e_{15}^{(2)}(\lambda_1\chi-\tilde{H}_{11})}{(\lambda_1\chi-\tilde{H}_{11})\left[c_{44}^{(2)}-(1-\eta^{(2)})\,\tilde{c}_{44}^{(2)}\right]} & i\dfrac{\tilde{H}_{12}-e_{15}^{(2)}(\lambda_2\chi-\tilde{H}_{11})}{\tilde{H}_{12}\left[c_{44}^{(2)}-(1-\eta^{(2)})\,\tilde{c}_{44}^{(2)}\right]} \\ i\dfrac{e_{15}^{(2)}\tilde{H}_{12}-\eta^{(2)}\tilde{c}_{44}^{(2)}\varepsilon_{11}^{(2)}(\lambda_1\chi-\tilde{H}_{11})}{(\lambda_1\chi-\tilde{H}_{11})\left[c_{44}^{(2)}-(1-\eta^{(2)})\,\tilde{c}_{44}^{(2)}\right]} & \dfrac{-e_{15}^{(2)}\tilde{H}_{12}+\eta^{(2)}\tilde{c}_{44}^{(2)}\varepsilon_{11}^{(2)}(\lambda_2\chi-\tilde{H}_{11})}{\tilde{H}_{12}\left[c_{44}^{(2)}-(1-\eta^{(2)})\,\tilde{c}_{44}^{(2)}\right]} \end{bmatrix}$$
$$\times\begin{bmatrix} it_{11}\exp\left[i\lambda_1(z-i\eta^{(1)}\delta)\right]E_1\left[i\lambda_1(z-i\eta^{(1)}\delta)\right]+it_{12}\exp\left[i\lambda_1(z-i\delta)\right]E_1\left[i\lambda_1(z-i\delta)\right] \\ t_{21}\exp\left[i\lambda_2(z-i\eta^{(1)}\delta)\right]E_1\left[i\lambda_2(z-i\eta^{(1)}\delta)\right]+t_{22}\exp\left[i\lambda_2(z-i\delta)\right]E_1\left[i\lambda_2(z-i\delta)\right] \end{bmatrix}. \tag{46}$$

Similarly, the above expressions of $\boldsymbol{f}_1'(z)$ and $\boldsymbol{f}_2'(z)$ are only valid along the real x-axis; however, it's not difficult to arrive at the full-field expressions of $\boldsymbol{f}_1'(z)$ and $\boldsymbol{f}_2'(z)$ which are listed in the appendix. Furthermore, the last term in $\boldsymbol{f}_1'(z)$ is the singular part due to the screw dislocation whilst the first two terms in $\boldsymbol{f}_1'(z)$ are the regular parts due to the existence of the compliant and highly conducting interface. Once $\boldsymbol{f}_1'(z)$ and $\boldsymbol{f}_2'(z)$ are known, the stresses, strains, electric displacements and electric fields can be obtained easily. For instance, the traction and tangential electric field along the compliant and highly conducting interface are as follows

$$\sigma_{32}=\mathrm{Im}\left\{\begin{aligned} &\frac{\tilde{H}_{12}t_{11}}{\tilde{H}_{11}-\lambda_1\chi}\exp\left[i\lambda_1(x-i\eta^{(1)}\delta)\right]E_1\left[i\lambda_1(x-i\eta^{(1)}\delta)\right] \\ &+\frac{\tilde{H}_{12}t_{12}}{\tilde{H}_{11}-\lambda_1\chi}\exp\left[i\lambda_1(x-i\delta)\right]E_1\left[i\lambda_1(x-i\delta)\right] \\ &-t_{21}\exp\left[i\lambda_2(x-\mathrm{i}\eta^{(1)}\delta)\right]E_1\left[\mathrm{i}\lambda_2(x-\mathrm{i}\eta^{(1)}\delta)\right] \\ &-t_{22}\exp\left[i\lambda_2(x-i\delta)\right]E_1\left[i\lambda_2(x-i\delta)\right] \end{aligned}\right\},$$
$$E_1=\mathrm{Re}\left\{\begin{aligned} &-t_{11}\exp\left[i\lambda_1(x-i\eta^{(1)}\delta)\right]E_1\left[i\lambda_1(x-i\eta^{(1)}\delta)\right] \\ &-t_{12}\exp\left[i\lambda_1(x-i\delta)\right]E_1\left[i\lambda_1(x-i\delta)\right] \\ &+\frac{(\tilde{H}_{11}-\lambda_2\chi)t_{21}}{\tilde{H}_{12}}\exp\left[i\lambda_2(x-i\eta^{(1)}\delta)\right]E_1\left[i\lambda_2(x-i\eta^{(1)}\delta)\right] \\ &+\frac{(\tilde{H}_{11}-\lambda_2\chi)t_{22}}{\tilde{H}_{12}}\exp\left[i\lambda_2(x-i\delta)\right]E_1\left[i\lambda_2(x-i\delta)\right] \end{aligned}\right\}, \quad \text{on } y=0. \tag{47}$$

Table 1 Material properties of PZT-5 and $BaTiO_3$ [16].

compound	c_{44} (10^{10} N/m^2)	e_{15} (C/m^2)	ε_{11} (10^{-9} F/m)	ρ (10^3 kg/m^3)	s (m/s)	c_{bg} (m/s)
PZT-5	2.11	12.3	8.1103	7.75	2264.9	2000.03
$BaTiO_3$	4.4	11.4	9.8722	5.7	3166.8	3081.7

4 Numerical examples

In this section, using the derived solution, we numerically investigate the influence of the interface imperfection and the velocity of the moving dislocation on the induced stresses and electric displacements in the piezoelectric bimaterial. The interface studied in the example is the first type, namely, a compliant and weakly conducting one. The upper half-plane is PZT-5 while the lower half-plane is $BaTiO_3$. The material properties of PZT-5 and $BaTiO_3$ are list below. In addition we assume that $\alpha = g\delta/c_{44}^{(1)}$ and $\beta = g\delta/(5\varepsilon_{11}^{(1)})$, where g is a dimensionless constant which characterizes the interface imperfection. Notice that a larger g represents a more compliant and more weakly conducting interface.

We demonstrate in Figs. 2 and 3 the variation of the normalized traction $\tilde{\sigma}_{32} = \sigma_{32}\delta/(c_{44}^{(1)}b)$ and the normalized normal electric displacement $\tilde{D}_2 = D_2\delta/(e_{15}^{(1)}b)$ along the positive real axis due to an elastic dislocation $b \neq 0$ and $\Delta\phi = 0$ at four different velocities $V = 0$, 1000, 1500, 2000 m/s and for four different interface values $g = 0.1$, 1, 10, 100. Apparently both the dislocation velocity and the interface imper-

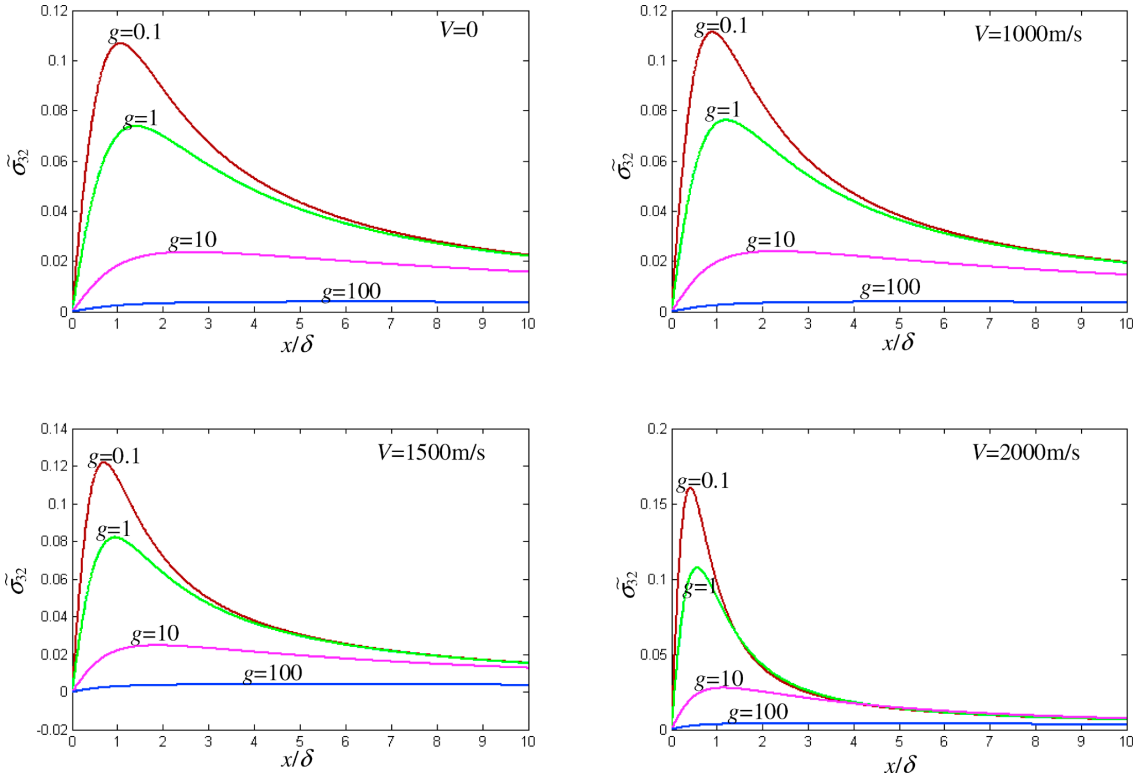

Fig. 2 (online colour at: www.pss-b.com) Variation of the normalized traction $\tilde{\sigma}_{32} = \sigma_{32}\delta/(c_{44}^{(1)}b)$ along the positive real axis due to an elastic dislocation $b \neq 0$ and $\Delta\phi = 0$ at four different velocities $V = 0$, 1000, 1500, 2000 m/s and for four different interface values $g = 0.1$, 1, 10, 100 (the upper half-plane is PZT-5 whilst the lower half-plane is $BaTiO_3$).

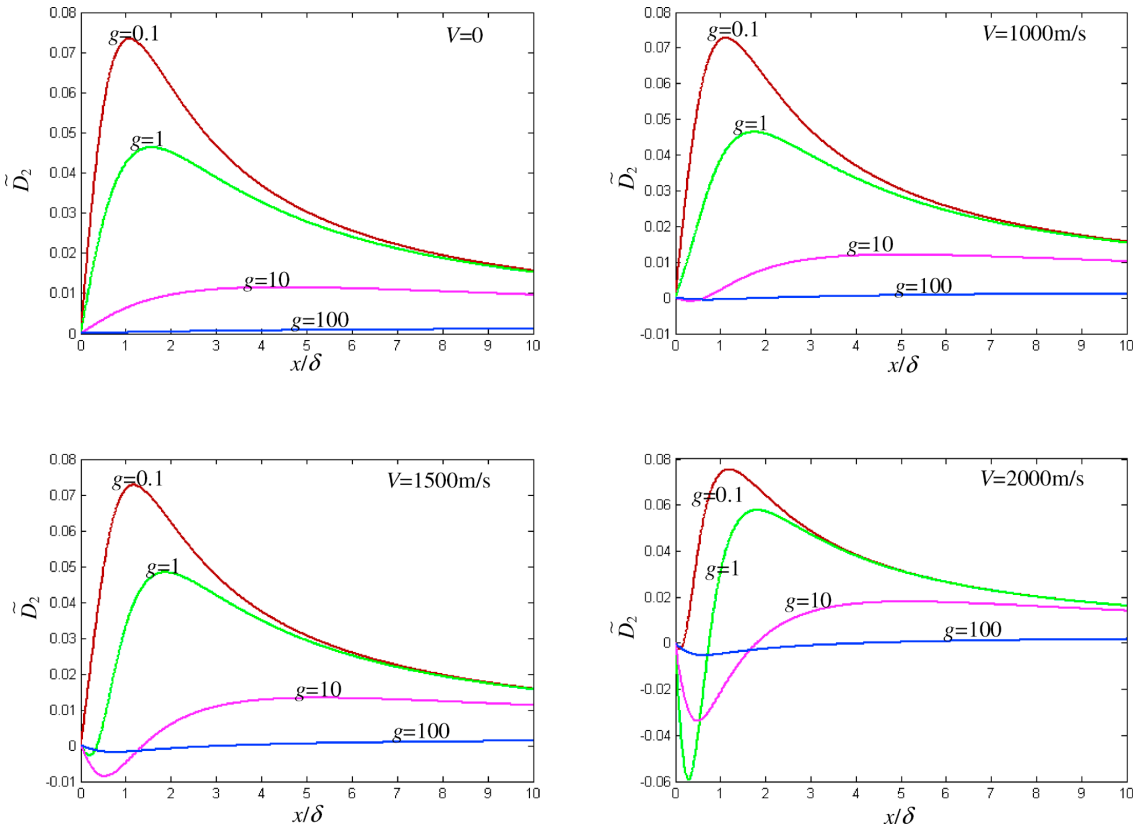

Fig. 3 (online colour at: www.pss-b.com) Variation of the normalized normal electric displacement $\tilde{D}_2 = D_2\delta/(e_{15}^{(1)}b)$ along the positive real axis due to an elastic dislocation $b \neq 0$ and $\Delta\phi = 0$ at four different velocities $V = 0$, 1000, 1500, 2000 m/s and for four different interface values $g = 0.1$, 1, 10, 100 (the upper half-plane is PZT-5 whilst the lower half-plane is $BaTiO_3$).

fection can significantly influence the distribution of the traction and normal electric displacement along the interface. For instance, with increasing dislocation velocity, the stress curves become steeper (Fig. 2). At a fixed velocity, the magnitude of the traction decreases with increasing g. It is observed from Fig. 3 that the normal electric displacement $\tilde{D}_2$ induced by a static elastic dislocation is always positive along the positive real axis; whilst at the other three higher velocities $V = 1000$, 1500, 2000 m/s, both negative and positive $\tilde{D}_2$ coexist. Most interestingly, when $V = 2000$ m/s, a medium value of g (i.e., $g = 1$ and 10 in Fig. 3) will cause a large negative domain for $\tilde{D}_2$ in the vicinity of the imperfect interface with the magnitude of the negative $\tilde{D}_2$ being further comparable to the positive one.

The full field distributions of stresses and electric displacements induced by the moving dislocation are illustrated in Figs. 4 and 5 where the contours of the normalized stress $\tilde{\sigma}_{32} = \sigma_{32}\delta/(c_{44}^{(1)}b)$ and the normalized electric displacement $\tilde{D}_2 = D_2\delta/(e_{15}^{(1)}b)$ are due to the elastic dislocation with $V = 2000$ m/s and $g = 1$. In both Figs. 4 and 5, the normalized x and y are defined as x/δ and y/δ, respectively, and the horizontal dashed line is used to denote the imperfect interface $y = 0$. It is apparent that due to the imperfect interface, both σ_{32} and D_2 are no longer symmetric with respect to the horizontal axis of the dislocation (x/δ =1); However, both the stress and electric displacement are continuous across the imperfect interface as expected. It is further noticed from Figs. 4 and 5 that while the magnitudes of σ_{32} and D_2 are very high near the dislocation (due to the singularity), a negative field domain exists for both quantities. Furthermore, we point out that while the negative domain for σ_{32} is associated with the localized dislocation behavior only (near the singularity, Fig. 4), that for D_2, which is in the vicinity of the interface

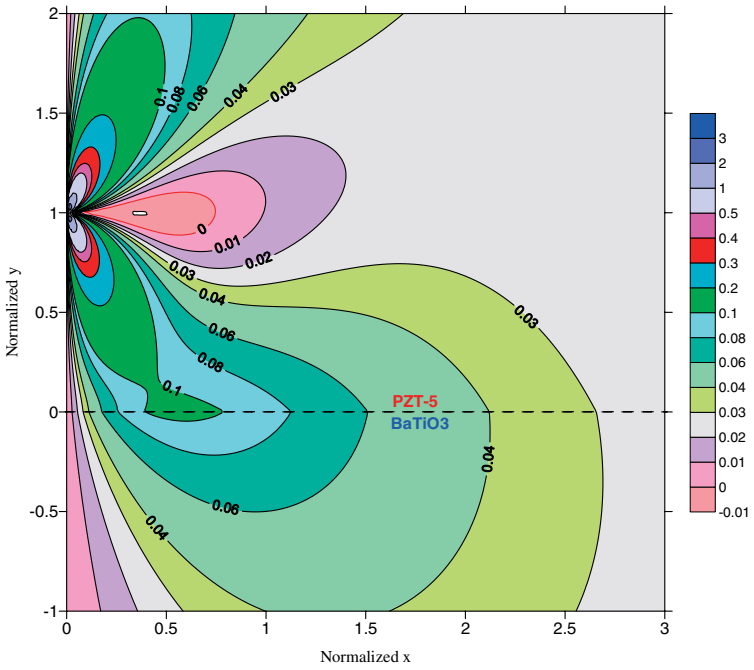

Fig. 4 (online colour at: www.pss-b.com) Contour plots of the normalized stress $\tilde{\sigma}_{32} = \sigma_{32}\delta/(c_{44}^{(1)}b)$ in the piezoelectric bimaterial due to an elastic dislocation $b \neq 0$ and $\Delta\phi = 0$ with $V = 2000$ m/s and $g = 1$ (the upper half-plane is PZT-5 whilst the lower half-plane is $BaTiO_3$).

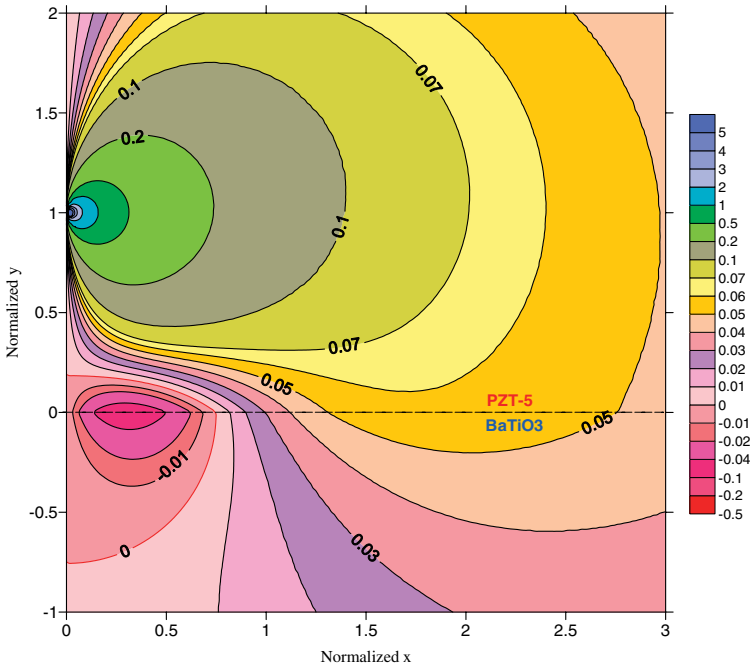

Fig. 5 (online colour at: www.pss-b.com) Contour plots of the normalized electric displacement $\tilde{D}_2 = D_2\delta/(e_{15}^{(1)}b)$ in the piezoelectric bimaterial due to an elastic dislocation $b \neq 0$ and $\Delta\phi = 0$ with $V = 2000$ m/s and $g = 1$ (the upper half-plane is PZT-5 whilst the lower half-plane is $BaTiO_3$).

(Fig. 5), is clearly caused by the interface imperfection. The variation of D_2 along the interface in Fig. 5 is also consistent with Fig. 3 for $V = 2000$ m/s.

5 Concluding remarks

We have derived exact closed-form solutions for a moving screw dislocation in a piezoelectric bimaterial with an imperfect interface. These solutions should be useful for analyzing the interaction between the interface imperfection and the velocity of the moving dislocation, and the corresponding impact on the involved material properties (e.g., [2, 4]). Numerical results are presented to verify the obtained solution and to demonstrate the significant influence of the interface imperfection and the velocity of the dislocation on the induced electroelastic fields. We remark that our solutions are valid for $V < \min\{c_{\text{bg}}^{(1)}, c_{\text{bg}}^{(2)}\}$. This condition is different from the condition $V < \min\{s^{(1)}, s^{(2)}\}$ for a perfect interface [7]. The solutions for the high velocity case $\min\{c_{\text{bg}}^{(1)}, c_{\text{bg}}^{(2)}\} < V < \min\{s^{(1)}, s^{(2)}\}$ need to be considered separately, which could be an interesting new topic.

Acknowledgements This work was supported in part by ARO/ARL and AFOSR/AFRL.

Appendix: The full-field expressions of $f_1'(z)$ and $f_2'(z)$

We can write $\boldsymbol{f}_1'(z)$ and $\boldsymbol{f}_2'(z)$ in the following forms

$$\boldsymbol{f}_1'(z) = \begin{bmatrix} P_1(z_1^{(1)}) \\ P_2(z) \end{bmatrix}, \qquad \boldsymbol{f}_2'(z) = \begin{bmatrix} Q_1(z_1^{(2)}) \\ Q_2(z) \end{bmatrix}, \tag{A1}$$

where $z_1^{(1)} = x + i\eta^{(1)} y$, $z_1^{(2)} = x + i\eta^{(2)} y$. When the interface is compliant and weakly conducting, the explicit expressions for $P_1(z_1^{(1)})$, $P_2(z)$, $Q_1(z_1^{(2)})$, $Q_2(z)$ are given by

$$\begin{aligned} P_1(z_1^{(1)}) = &- \frac{ik_{11}\left[\varepsilon_{11}^{(1)} H_{12} + e_{15}^{(1)}(\lambda_1\alpha - H_{11})\right]}{\eta^{(1)}\tilde{c}_{44}^{(1)}\varepsilon_{11}^{(1)}(\lambda_1\alpha - H_{11})} \exp\left[-i\lambda_1(z_1^{(1)} + i\eta^{(1)}\delta)\right] E_1\left[-i\lambda_1(z_1^{(1)} + i\eta^{(1)}\delta)\right] \\ &- \frac{ik_{12}\left[\varepsilon_{11}^{(1)} H_{12} + e_{15}^{(1)}(\lambda_1\alpha - H_{11})\right]}{\eta^{(1)}\tilde{c}_{44}^{(1)}\varepsilon_{11}^{(1)}(\lambda_1\alpha - H_{11})} \exp\left[-i\lambda_1(z_1^{(1)} + i\delta)\right] E_1\left[-i\lambda_1(z_1^{(1)} + i\delta)\right] \\ &- \frac{ik_{21}\left[\varepsilon_{11}^{(1)} H_{12} + e_{15}^{(1)}(\lambda_2\alpha - H_{11})\right]}{\eta^{(1)}\tilde{c}_{44}^{(1)}\varepsilon_{11}^{(1)} H_{12}} \exp\left[-i\lambda_2(z_1^{(1)} + i\eta^{(1)}\delta)\right] E_1\left[-i\lambda_2(z_1^{(1)} + i\eta^{(1)}\delta)\right] \\ &- \frac{ik_{22}\left[\varepsilon_{11}^{(1)} H_{12} + e_{15}^{(1)}(\lambda_2\alpha - H_{11})\right]}{\eta^{(1)}\tilde{c}_{44}^{(1)}\varepsilon_{11}^{(1)} H_{12}} \exp\left[-i\lambda_2(z_1^{(1)} + i\delta)\right] E_1\left[-i\lambda_2(z_1^{(1)} + i\delta)\right] \\ &- \frac{b}{2\pi(z_1^{(1)} + i\eta^{(1)}\delta)} + \frac{b}{2\pi(z_1^{(1)} - i\eta^{(1)}\delta)}, \end{aligned} \tag{A2}$$

$$\begin{aligned} P_2(z) = &\frac{ik_{11}}{\varepsilon_{11}^{(1)}} \exp\left[-i\lambda_1(z + i\eta^{(1)}\delta)\right] E_1\left[-i\lambda_1(z + i\eta^{(1)}\delta)\right] \\ &+ \frac{ik_{12}}{\varepsilon_{11}^{(1)}} \exp\left[-i\lambda_1(z + i\delta)\right] E_1\left[-i\lambda_1(z + i\delta)\right] \\ &+ \frac{ik_{21}(\lambda_2\alpha - H_{11})}{\varepsilon_{11}^{(1)} H_{12}} \exp\left[-i\lambda_2(z + i\eta^{(1)}\delta)\right] E_1\left[-i\lambda_2(z + i\eta^{(1)}\delta)\right] \\ &+ \frac{ik_{22}(\lambda_2\alpha - H_{11})}{\varepsilon_{11}^{(1)} H_{12}} \exp\left[-i\lambda_2(z + i\delta)\right] E_1\left[-i\lambda_2(z + i\delta)\right] - \frac{\varepsilon_{11}^{(1)}\Delta\phi - e_{15}^{(1)} b}{2\pi\varepsilon_{11}^{(1)}(z + \mathrm{i}\delta)} + \frac{\varepsilon_{11}^{(1)}\Delta\phi - e_{15}^{(1)} b}{2\pi\varepsilon_{11}^{(1)}(z - \mathrm{i}\delta)}, \end{aligned} \tag{A3}$$

$$
\begin{aligned}
Q_1(z_1^{(2)}) = {} & \frac{ik_{11}\left[\varepsilon_{11}^{(2)}H_{12}+e_{15}^{(2)}(\lambda_1\alpha-H_{11})\right]}{\eta^{(2)}\tilde{c}_{44}^{(2)}\varepsilon_{11}^{(2)}(\lambda_1\alpha-H_{11})}\exp\left[i\lambda_1(z_1^{(2)}-\mathrm{i}\eta^{(1)}\delta)\right]E_1\left[i\lambda_1(z_1^{(2)}-i\eta^{(1)}\delta)\right] \\
& + \frac{ik_{12}\left[\varepsilon_{11}^{(2)}H_{12}+e_{15}^{(2)}(\lambda_1\alpha-H_{11})\right]}{\eta^{(2)}\tilde{c}_{44}^{(2)}\varepsilon_{11}^{(2)}(\lambda_1\alpha-H_{11})}\exp\left[i\lambda_1(z_1^{(2)}-i\delta)\right]E_1\left[i\lambda_1(z_1^{(2)}-i\delta)\right] \\
& + \frac{ik_{21}\left[\varepsilon_{11}^{(2)}H_{12}+e_{15}^{(2)}(\lambda_2\alpha-H_{11})\right]}{\eta^{(2)}\tilde{c}_{44}^{(2)}\varepsilon_{11}^{(2)}H_{12}}\exp\left[i\lambda_2(z_1^{(2)}-i\eta^{(1)}\delta)\right]E_1\left[i\lambda_2(z_1^{(2)}-i\eta^{(1)}\delta)\right] \\
& + \frac{ik_{22}\left[\varepsilon_{11}^{(2)}H_{12}+e_{15}^{(2)}(\lambda_2\alpha-H_{11})\right]}{\eta^{(2)}\tilde{c}_{44}^{(2)}\varepsilon_{11}^{(2)}H_{12}}\exp\left[i\lambda_2(z_1^{(2)}-i\delta)\right]E_1\left[i\lambda_2(z_1^{(2)}-i\delta)\right], \qquad \text{(A4)}
\end{aligned}
$$

$$
\begin{aligned}
Q_2(z) = {} & -\frac{ik_{11}}{\varepsilon_{11}^{(2)}}\exp\left[i\lambda_1(z-i\eta^{(1)}\delta)\right]E_1\left[i\lambda_1(z-i\eta^{(1)}\delta)\right] \\
& - \frac{ik_{12}}{\varepsilon_{11}^{(2)}}\exp\left[i\lambda_1(z-i\delta)\right]E_1\left[i\lambda_1(z-i\delta)\right] \\
& + \frac{ik_{21}(H_{11}-\lambda_2\alpha)}{\varepsilon_{11}^{(2)}H_{12}}\exp\left[i\lambda_2(z-i\eta^{(1)}\delta)\right]E_1\left[i\lambda_2(z-i\eta^{(1)}\delta)\right] \\
& + \frac{ik_{22}(H_{11}-\lambda_2\alpha)}{\varepsilon_{11}^{(2)}H_{12}}\exp\left[i\lambda_2(z-i\delta)\right]E_1\left[i\lambda_2(z-i\delta)\right]. \qquad \text{(A5)}
\end{aligned}
$$

When the interface is compliant and highly conducting, the explicit expressions for $P_1(z_1^{(1)})$, $P_2(z)$, $Q_1(z_1^{(2)})$, $Q_2(z)$ are given by

$$
\begin{aligned}
P_1(z_1^{(1)}) = {} & -\frac{it_{11}\left[\tilde{H}_{12}+e_{15}^{(1)}(\lambda_1\chi-\tilde{H}_{11})\right]}{(\lambda_1\chi-\tilde{H}_{11})\left[c_{44}^{(1)}-(1-\eta^{(1)})\,\tilde{c}_{44}^{(1)}\right]}\exp\left[-i\lambda_1(z_1^{(1)}+i\eta^{(1)}\delta)\right]E_1\left[-i\lambda_1(z_1^{(1)}+i\eta^{(1)}\delta)\right] \\
& - \frac{it_{12}\left[\tilde{H}_{12}+e_{15}^{(1)}(\lambda_1\chi-\tilde{H}_{11})\right]}{(\lambda_1\chi-\tilde{H}_{11})\left[c_{44}^{(1)}-(1-\eta^{(1)})\,\tilde{c}_{44}^{(1)}\right]}\exp\left[-i\lambda_1(z_1^{(1)}+i\delta)\right]E_1\left[-i\lambda_1(z_1^{(1)}+i\delta)\right] \\
& - \frac{it_{21}\left[\tilde{H}_{12}+e_{15}^{(1)}(\lambda_2\chi-\tilde{H}_{11})\right]}{\tilde{H}_{12}\left[c_{44}^{(1)}-(1-\eta^{(1)})\,\tilde{c}_{44}^{(1)}\right]}\exp\left[-i\lambda_2(z_1^{(1)}+i\eta^{(1)}\delta)\right]E_1\left[-i\lambda_2(z_1^{(1)}+i\eta^{(1)}\delta)\right] \\
& - \frac{it_{22}\left[\tilde{H}_{12}+e_{15}^{(1)}(\lambda_2\chi-\tilde{H}_{11})\right]}{\tilde{H}_{12}\left[c_{44}^{(1)}-(1-\eta^{(1)})\,\tilde{c}_{44}^{(1)}\right]}\exp\left[-i\lambda_2(z_1^{(1)}+i\delta)\right]E_1\left[-i\lambda_2(z_1^{(1)}+i\delta)\right] \\
& - \frac{\left[(1+\eta^{(1)})\,\tilde{c}_{44}^{(1)}-c_{44}^{(1)}\right]b}{2\pi\left[c_{44}^{(1)}-(1-\eta^{(1)})\,\tilde{c}_{44}^{(1)}\right](z_1^{(1)}+i\eta^{(1)}\delta)} - \frac{e_{15}^{(1)}(\varepsilon_{11}^{(1)}\,\Delta\phi-e_{15}^{(1)}b)}{\pi\varepsilon_{11}^{(1)}\left[c_{44}^{(1)}-(1-\eta^{(1)})\,\tilde{c}_{44}^{(1)}\right](z_1^{(1)}+i\delta)} \\
& + \frac{b}{2\pi(z_1^{(1)}-i\eta^{(1)}\delta)}, \qquad \text{(A6)}
\end{aligned}
$$

$$
\begin{aligned}
P_2(z) = {} & \frac{t_{11}\left[e_{15}^{(1)}\tilde{H}_{12}+\eta^{(1)}\tilde{c}_{44}^{(1)}\varepsilon_{11}^{(1)}(\lambda_1\chi-\tilde{H}_{11})\right]}{(\lambda_1\chi-\tilde{H}_{11})\left[c_{44}^{(1)}-(1-\eta^{(1)})\,\tilde{c}_{44}^{(1)}\right]}\exp\left[-i\lambda_1(z+i\eta^{(1)}\delta)\right]E_1\left[-i\lambda_1(z+i\eta^{(1)}\delta)\right] \\
& + \frac{t_{12}\left[e_{15}^{(1)}\tilde{H}_{12}+\eta^{(1)}\tilde{c}_{44}^{(1)}\varepsilon_{11}^{(1)}(\lambda_1\chi-\tilde{H}_{11})\right]}{(\lambda_1\chi-\tilde{H}_{11})\left[c_{44}^{(1)}-(1-\eta^{(1)})\,\tilde{c}_{44}^{(1)}\right]}\exp\left[-i\lambda_1(z+i\delta)\right]E_1\left[-i\lambda_1(z+i\delta)\right] \\
& + \frac{t_{21}\left[e_{15}^{(1)}\tilde{H}_{12}+\eta^{(1)}\tilde{c}_{44}^{(1)}\varepsilon_{11}^{(1)}(\lambda_2\chi-\tilde{H}_{11})\right]}{\tilde{H}_{12}\left[c_{44}^{(1)}-(1-\eta^{(1)})\,\tilde{c}_{44}^{(1)}\right]}\exp\left[-i\lambda_2(z+i\eta^{(1)}\delta)\right]E_1\left[-i\lambda_2(z+i\eta^{(1)}\delta)\right]
\end{aligned}
$$

$$+\frac{t_{22}\left[e_{15}^{(1)}\tilde{H}_{12}+\eta^{(1)}\tilde{c}_{44}^{(1)}\varepsilon_{11}^{(1)}(\lambda_2\chi-\tilde{H}_{11})\right]}{\tilde{H}_{12}\left[c_{44}^{(1)}-(1-\eta^{(1)})\,\tilde{c}_{44}^{(1)}\right]}\exp\left[-i\lambda_2(z+i\delta)\right]E_1\left[-i\lambda_2(z+i\delta)\right]$$
$$-\frac{i\eta^{(1)}\tilde{c}_{44}^{(1)}e_{15}^{(1)}b}{\pi\left[c_{44}^{(1)}-(1-\eta^{(1)})\,\tilde{c}_{44}^{(1)}\right](z+i\eta^{(1)}\delta)}-\frac{i\left[(1+\eta^{(1)})\,\tilde{c}_{44}^{(1)}-c_{44}^{(1)}\right](\varepsilon_{11}^{(1)}\,\Delta\phi-e_{15}^{(1)}b)}{2\pi\left[c_{44}^{(1)}-(1-\eta^{(1)})\,\tilde{c}_{44}^{(1)}\right](z+\mathrm{i}\delta)}$$
$$+\frac{i(e_{15}^{(1)}b-\varepsilon_{11}^{(1)}\,\Delta\phi)}{2\pi(z-i\delta)}, \tag{A7}$$

$$Q_1(z_1^{(2)})=\frac{it_{11}\left[\tilde{H}_{12}-e_{15}^{(2)}(\lambda_1\chi-\tilde{H}_{11})\right]}{(\lambda_1\chi-\tilde{H}_{11})\left[c_{44}^{(2)}-(1-\eta^{(2)})\,\tilde{c}_{44}^{(2)}\right]}\exp\left[i\lambda_1(z_1^{(2)}-i\eta^{(1)}\delta)\right]E_1\left[i\lambda_1(z_1^{(2)}-i\eta^{(1)}\delta)\right]$$
$$+\frac{it_{12}\left[\tilde{H}_{12}-e_{15}^{(2)}(\lambda_1\chi-\tilde{H}_{11})\right]}{(\lambda_1\chi-\tilde{H}_{11})\left[c_{44}^{(2)}-(1-\eta^{(2)})\,\tilde{c}_{44}^{(2)}\right]}\exp\left[i\lambda_1(z_1^{(2)}-i\delta)\right]E_1\left[i\lambda_1(z_1^{(2)}-i\delta)\right]$$
$$+\frac{it_{21}\left[\tilde{H}_{12}-e_{15}^{(2)}(\lambda_2\chi-\tilde{H}_{11})\right]}{\tilde{H}_{12}\left[c_{44}^{(2)}-(1-\eta^{(2)})\,\tilde{c}_{44}^{(2)}\right]}\exp\left[i\lambda_2(z_1^{(2)}-i\eta^{(1)}\delta)\right]E_1\left[i\lambda_2(z_1^{(2)}-i\eta^{(1)}\delta)\right]$$
$$+\frac{it_{22}\left[\tilde{H}_{12}-e_{15}^{(2)}(\lambda_2\chi-\tilde{H}_{11})\right]}{\tilde{H}_{12}\left[c_{44}^{(2)}-(1-\eta^{(2)})\,\tilde{c}_{44}^{(2)}\right]}\exp\left[i\lambda_2(z_1^{(2)}-i\delta)\right]E_1\left[i\lambda_2(z_1^{(2)}-i\delta)\right], \tag{A8}$$

$$Q_2(z)=\frac{t_{11}\left[\eta^{(2)}\tilde{c}_{44}^{(2)}\varepsilon_{11}^{(2)}(\lambda_1\chi-\tilde{H}_{11})-e_{15}^{(2)}\tilde{H}_{12}\right]}{(\lambda_1\chi-\tilde{H}_{11})\left[c_{44}^{(2)}-(1-\eta^{(2)})\,\tilde{c}_{44}^{(2)}\right]}\exp\left[i\lambda_1(z-i\eta^{(1)}\delta)\right]E_1\left[i\lambda_1(z-i\eta^{(1)}\delta)\right]$$
$$+\frac{t_{12}\left[\eta^{(2)}\tilde{c}_{44}^{(2)}\varepsilon_{11}^{(2)}(\lambda_1\chi-\tilde{H}_{11})-e_{15}^{(2)}\tilde{H}_{12}\right]}{(\lambda_1\chi-\tilde{H}_{11})\left[c_{44}^{(2)}-(1-\eta^{(2)})\,\tilde{c}_{44}^{(2)}\right]}\exp\left[i\lambda_1(z-i\delta)\right]E_1\left[i\lambda_1(z-i\delta)\right]$$
$$+\frac{t_{21}\left[\eta^{(2)}\tilde{c}_{44}^{(2)}\varepsilon_{11}^{(2)}(\lambda_2\chi-\tilde{H}_{11})-e_{15}^{(2)}\tilde{H}_{12}\right]}{\tilde{H}_{12}\left[c_{44}^{(2)}-(1-\eta^{(2)})\,\tilde{c}_{44}^{(2)}\right]}\exp\left[i\lambda_2(z-i\eta^{(1)}\delta)\right]E_1\left[i\lambda_2(z-i\eta^{(1)}\delta)\right]$$
$$+\frac{t_{22}\left[\eta^{(2)}\tilde{c}_{44}^{(2)}\varepsilon_{11}^{(2)}(\lambda_2\chi-\tilde{H}_{11})-e_{15}^{(2)}\tilde{H}_{12}\right]}{\tilde{H}_{12}\left[c_{44}^{(2)}-(1-\eta^{(2)})\,\tilde{c}_{44}^{(2)}\right]}\exp\left[i\lambda_2(z-i\delta)\right]E_1\left[i\lambda_2(z-i\delta)\right]. \tag{A9}$$

References

[1] G. Schoeck, Phys. Rev. **102**, 1458 (1956).
[2] W. G. Johnston and J. J. Gilman, J. Appl. Phys. **30**, 129 (1959).
[3] W. G. Johnston and J. J. Gilman, J. Appl. Phys. **31**, 632 (1960).
[4] H. Koizumi, H. O. K. Kirchner, and T. Suzuki, Phys. Rev. B **65**, 214104 (2002).
[5] X. Wang and Z. Zhong, Mech. Res. Commun. **29**, 425 (2002).
[6] X. F. Wu, Y. A. Dzenis, and W. S. Zou, phys. stat. sol. (b) **238**, 120 (2003).
[7] J. X. Liu and D. N. Fang, phys. stat. sol. (b) **241**, 962 (2004).
[8] A. K. Soh, J. X. Liu, K. L. Lee, and D. N. Fang, phys. stat. sol. (b) **242**, 842 (2005).
[9] J. S. Yang, Acta Mech. **172**, 123 (2004).
[10] J. Aboudi, Compos. Sci. Technol. **28**, 103 (1987).
[11] H. Fan and K. Y. Sze, Mech. Mater. **33**, 363 (2001).
[12] X. Wang and L. J. Sudak, Int. J. Solids Struct., in press (available online, 2006).
[13] H. Fan, J. S. Yang, and L. M. Xu, Appl. Phys. Lett. **88**, 203509 (2006).
[14] A. N. Stroh, J. Math. Phys. **41**, 77 (1962).

[15] W. Yang, Z. Suo, and C. F. Shih, Proc. R. Soc. Lond. A **433**, 679 (1991).
[16] X. Wang, Z. Zhong, and F. L. Wu, Int. J. Solids Struct. **40**, 2381 (2003).
[17] D. L. Clements, Int. J. Eng. Sci. **9**, 257 (1971).
[18] J. L. Bleustein, Appl. Phys. Lett. **13**, 412 (1968).
[19] Y. V. Gulyaev, Sov. Phys. JETP **9**, 37 (1969).
[20] M. Abramovitz and I. A. Stegun (eds.), Handbook of Mathematical Functions with Formulas, Graphs, and Mathematical Tables (Dover, New York, 1972).

